Purpose or Objective: The study aims at evaluating the dosimetric effect of the metal artifact reduction (MAR) function for three different types of dose calculation algorithms in H&N radiotherapy.

Material and Methods: A virtual H&N patient (vH&N) was designed based on a round-shaped dosimetric phantom (cheese phantom). Two types of metal (tungsten 4.59g/cm3 and Cerrobend alloy 9.4g/cm3: Ø3 cm) were inserted into the vH&N to simulate an H&N patient with dental prosthesis. We obtained two types of CT image sets with MAR-on and MAR-off conditions and imported a contour set for the PTV, parotid, and spinal cord, which from a Nasopharynx case. An IMRT with five step & shoot beams was created for the MAR-off CT image set using the Monte Carlo dose calculation algorithm (MC, iPlan, BrainLAB) by following RTOG1197 guidelines. Two different plans were calculated by applying pencil beam (PB) and collapsed cone convolution (CCC) dose calculation algorithms with the same beam parameters and MLC shape. The same procedure was applied to the MAR-on CT image set. A total of six plans with the same beam parameters were generated. We calculated dose at five points of interest and compared with the doses measured at the same points. The 2D axial dose distribution was evaluated through film dosimetry by applying Gamma analysis with 3 mm and 3% criteria for all plans.

Results: The differences between the measured and calculated doses at the five points of interest for the MAR-on CT image set were significantly low compared to those for the MAR-off CT image set in all dose calculation algorithms (-1.6±1.8 vs -5.8±9%). The dose differences were the lowest in MC followed by CCC and PB. The most significant dose difference between MAR-on and MAR-off was observed in PB followed by MC and CCC. In the gamma analysis, the mean pass rate was significantly high in MAR-on compared to that in MAR-off (89.8±8 vs 61.6±16%). The pass rate was the highest in MC followed by CCC and PB. The most significant pass rate difference between MAR-on and MAR-off was observed in CCC (91.8 vs 45.4%) followed by MC (96.7 vs 62.3%) and PB (81.1 vs 77.1%).

		MAR on	MAR off
Measured dose difference		-1.6±1.8	-5.8±9
Gamma pass rate	MC	96.7	62.3
	CCC	91.8	45.4
	PB	81.1	77.1
	Overall	89.8±8	61.6±16

[Table 1] Measured dose differences and Gamma pass rates (%)

Conclusion: The dose calculation results with the MAR-on CT image set and MC showed better fit to measured data compared to the MAR-off CT image set with the other dose calculation algorithms. PB was more sensitive to metal artifacts for dose calculation of H&N followed by MC and CCC. MAR-on could thus provide a more realistic dose distribution for H&N with metal prosthesis.

EP-1836

HU to electron density conversion with virtual monochromatic images generated by dual-energy CT

V. González-Pérez[1], A. Bartrés[1], E. Arana[2], V. Crispín[1], V. De los Dolores[1], V. Campo[1], L. Oliver[1]
[1]Fundación Instituto Valenciano de Oncología, Servicio de Radiofísica y Protección Radiológica., Valencia, Spain
[2]Fundación Instituto Valenciano de Oncología, Servicio de Radiología, Valencia, Spain

Purpose or Objective: To assess dual-energy CT (DECT) and Metal Artefact Reduction algorithm (MAR) for radiotherapy planning. In particular, conversion of HU to electron density is evaluated in terms of monochromatic energy and the use of MAR in the presence of metal materials.

Material and Methods: Dual energy CT was performed using a Discovery CT750 HD scanner (GE Healthcare, USA). The DECTs were performed using fast kV-switching gemstone spectral imaging (GSI) between 80 kV and 140 kV. The CT data were reconstructed both with and without MAR to the monochromatic energies of 60 keV, 90 keV and 120 keV.
CIRS phantom model 062 (CIRS Inc., USA) was used to calibrate HU to electron density in that set of monochromatic energies. Two additional sets of CT were performed after including a home-made steel insert both on the periphery and in the center of the phantom, and different images were compared in the presence of artefacts.

Results: Different calibrations for monochromatic energies showed good HU to electron density linear correlation in all cases (R^2 ranging from 0.91 to 0.998). Linearity was better for higher virtual monochromatic energies. The slope maximum change in HU to electron density curves was 24.4% when comparing polienergetic "standard" CT with 120 keV virtual image. For monochromatic energy curve calibrations, differences are up to 38.0% between 60 and 120 keV monochromatic energy.
No significant differences were found in calibrations between using MAR or not. The maximum slope change in HU to electron density curves was 2.4% for 120 keV monochromatic images after MAR reconstruction.
The maximum change of the HU of an insert after the inclusion of artefacts was of 34,0 HU for 120 keV monochromatic energy compared to 50.7 HU for a conventional CT (Figure 1).

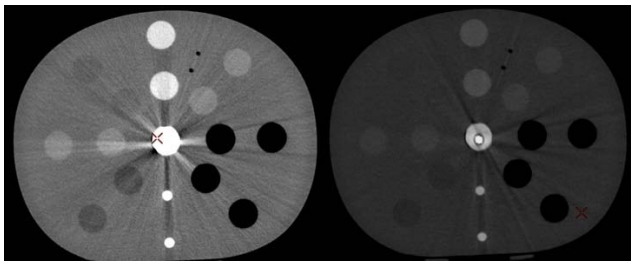

Figure 1: CIRS 062 Phantom used for HU to electron density conversion after inclusion of a steel-made insert at the phantom center. Standard polienergetic CT image (left) and monochromatic 120 keV (right)

Conclusion: The reduction of metal-related artefacts is improved at high monochromatic energies due to both the decrease of beam hardening effect and the use of MAR algortihm.
Therefore, using high keV monochromatic DECT virtual images and MAR algorithm is technically viable in radiotherapy planning since HU to electron density calibrations are feasible with monochromatic DECT image. DICOM standard is used for monochromatic virtual images and they were successfully exported to XiO treatment planning system (Elekta, Crawley, UK).

EP-1837

Impact on patient positioning using four CT datasets for image registration with CBCTs in lung SBRT

M. Oechsner[1], B. Chizzali[1], J.J. Wilkens[1,2], S.E. Combs[1,2], M.N. Duma[1,2]
[1]Klinikum Rechts der Isar- TU München, Department of Radiation Oncology, München, Germany
[2]Institute of Innovative Radiotherapy- Helmholtz Zentrum München, Department of Radiation Sciences, München, Germany

Purpose or Objective: A variety of CT datasets are available in lung stereotactic body radiotherapy (SBRT) for defining the target volume or treatment planning, e.g. slow planning CT (PCT), average intensity projection (AIP), maximum intensity projection (MIP) or mid-ventilation CT (MidV). The aim of this retrospective patient study was to evaluate the differences of using these four CT datasets for image registration with free breathing cone beam CTs (CBCT). Couch shifts between

the registrations were analyzed and correlated to different factors, e.g. tumor motion, size and location.

Material and Methods: CT datasets of 47 lung SBRT patients were retrospectively selected for this study. All patients had a PCT and a 4DCT scan. AIP and MIP CT datasets were calculated from the 10 phases of the 4DCTs. Additionally, a MidV CT was selected for each patient representing the mean position of the tumor. These four CT datasets were retrospectivlly registered to free breathing CBCTs which were acquired before patients' first treatments. Automatic image registration was performed with the Eclipse 13.0 registration software (Varian). 3D translational registrations were applied and the coordinates in left-right (x), anterior-posterior (y) and superior-inferior (z) direction were evaluated. Coordinates of each of the registered four CT datasets were compared to the coordinates of the other registered CT datasets (e.g. PCT-CBCT vs MIP-CBCT). Additionally, a 3D movement vector was calculated. Furthermore, we searched for correlations between registration differences and tumour parameters: 3D motion of the tumor, GTV volume and the distance between the carina of trachea and the GTV in z-direction (SI position). The Wilcoxon test was used to identify statistically significant difference between the fusion pairs (p-value <0.05). Correlations were analyzed using Spearman's rank correlation (rs).

Results: The table depicts median, minimal and maximal registration differences in x, y, z, and 3D direction between the CT datasets. Some differences were statistically significant (p<0.05). AIP-CBCT and MIP-CBCT achieved the smallest differences. The largest difference in 3D direction was observed for MIP-CBCT vs MidV-CBCT (10.5 mm). The figure depicts the frequency of shifts in 1 mm step sizes between the image registrations. Only 3D tumor motion showed a good correlation to the registration differences between AIP-CBCT and MIP-CBCT (rs: 0.73) or MIP-CBCT and MidV-CBCT (rs: 0.70).

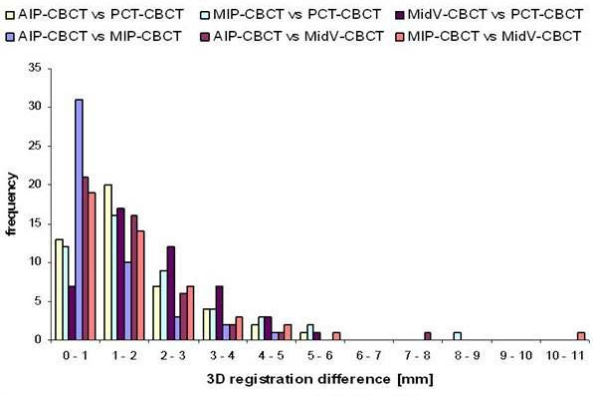

Δ couch shifts
median (min / max)

registration	Δx [mm]	Δy [mm]	Δz [mm]	Δ3D [mm]
AIP-CBCT vs PCT-CBCT	-0.5 (-2.1 / 2.7)	-0.1 (-2.9 / 2.2)	0.0 (-5.1 / 3.2)	1.4 (0.3 / 5.6)
MIP-CBCT vs PCT-CBCT	-0.5 (-1.3 / 2.9)	-0.4 (-4.0 / 1.8)	-0.3 (-8.7 / 3.3)	1.8 (0.4 / 8.8)
MidV-CBCT vs PCT-CBCT	-0.4 (2.0 / 2.2)	0.0 (-2.9 / 3.9)	-0.4 (-3.9 / 5.8)	1.9 (0.2 / 5.9)
AIP-CBCT vs MIP-CBCT	-0.1 (-1.0 / 1.2)	0.3 (-0.8 / 1.5)	0.1 (-3.0 / 4.3)	0.5 (0.1 / 4.4)
AIP-CBCT vs MidV-CBCT	-0.1 (-3.8 / 1.6)	-0.2 (-2.8 / 2.3)	0.2 (-6.3 / 2.7)	1.1 (0.1 / 7.6)
MIP-CBCT vs MidV-CBCT	-0.2 (-2.8 / 1.6)	-0.5 (-2.8 / 2.2)	0.0 (-9.9 / 5.7)	1.3 (0.1 / 10.5)

Conclusion: Using different CT datasets for image registration with free breathing CBCTs can result in distinctly different couch shifts. Automatic AIP-CBCT and MIP-CBCT fusion achieved the best agreement. Differences > 5mm were observed, which can be larger than the safety margins. This has to be considered if the CT dataset for treatment planning and image registration is chosen.

EP-1838

Proton therapy planning for brain tumors using MRI-generated PseudoCT

J. Seco[1], D. Izquierdo[2], C. Catana[2], G. Pileggi[3], J. Pursley[1], C. Speier[1,4], G. Sharp[1], C. Bert[4], C. Collins-Fekete[1], M.F. Spadea[3]
[1]*Massachusetts General Hospital Harvard Medical School, Radiation Oncology, Boston, USA*
[2]*Massachusetts General Hospital, Athinoula A. Martinos Center for Biomedical Imaging, Boston, USA*
[3]*Magna Graecia University, ImagEngLab and Experimental and Clinical Oncology, Catanzaro, Italy*
[4]*Friedrich-Alexander Universität Erlangen-Nürnberg, Radiation Oncology, Erlangen, Germany*

Purpose or Objective: To investigate the dosimetric and range accuracy of using MRI pseudoCT for proton therapy planning vs. single energy x-ray CT, for brain tumors.

Material and Methods: A cohort of 15 gliobastoma patients with CT and MRI (T1 and T2) imaged after surgical resection. T1-weighted 3D-MPRAGE was used to delineate the GTV, which was subsequently rigidly registered to the CT volume. A pseudoCT was generated from the aligned MRI by combining segmentation- and atlas-based approaches. The spatial resolution both for pseudo- and real CT was 0.6x0.6x2.5mm. Three orthogonal proton beams were simulated on the pseudo CT. Two co-planar beams were set on the axial plane. The third one was planned parallel to the cranio-caudal (CC) direction. Each beam was set to cover the GTV at 98% of the nominal dose (18Gy). The proton plan was copied and transferred to the real CT, including aperture/compensator geometry. Dose comparison between pseudoCT and CT plan was performed beam-by-beam by quantifying the range shift of dose profile on each slice of the GTV. The GTV's relative V98 was computed for the CT.

Results: For beams in axial plane the median absolute value of the range shift was 0.3mm, with 0.9mm and 1.4mm as 95th percentile and maximum, respectively. Worst scenarios were found for the CC beam, where we measured 1.1mm (median), 2.7mm (95th-percentile) and 5mm (maximum). Regardless the direction, beams passing through the surgical site, where metal (Titanium MRI compatible) staples were present, were mostly affected by range shift. GTV's V98 for CT was not lower than 99.3%.

Conclusion: The study showed the feasibility of an MRI-alone based proton plan. Advantages include the possibility to rely on better soft tissue contrast for target and organs at risk delineation without the need of further CT scan and image registration. Additional investigation is required in presence of metal implants along the beam path and to account for partial volume effects due to slice thickness.

EP-1839

exploiting planning CT data for accurate WEPL on CBCT reconstructions used in adaptive radiotherapy

J.H. Mason[1], M.E. Davies[1], W.H. Nailon[2]
[1]*University of Edinburgh, Institute for Digital Communications, Edinburgh, United Kingdom*
[2]*Edinburgh Cancer Centre- Western General Hospital, Department of Oncology Physics, Edinburgh, United Kingdom*

Purpose or Objective: To allow the use of cone beam computerised tomographic (CBCT) imaging for adaptive radiotherapy, its quantitative accuracy must be improved. However, since it is physically hindered by data insufficiency and large scatter contributions, this a difficult task without incorporating additional information. Here we propose a framework for utilising planning CT images within the reconstruction process to significantly improve the accuracy of CBCT and illustrate its potential use in proton therapy.